

Replication of Murine Coronavirus Defective Interfering RNA from Negative-Strand Transcripts

MYUNGSOO JOO,[†] SANGEETA BANERJEE, AND SHINJI MAKINO*

*Department of Microbiology, The University of Texas at Austin,
Austin, Texas 78712-1095*

Received 22 January 1996/Accepted 20 May 1996

The positive-strand defective interfering (DI) RNA of the murine coronavirus mouse hepatitis virus (MHV), when introduced into MHV-infected cells, results in DI RNA replication and accumulation. We studied whether the introduction of negative-strand transcripts of MHV DI RNA would also result in replication. At a location downstream of the T7 promoter and upstream of the human hepatitis delta virus ribozyme domain, we inserted a complete cDNA clone of MHV DI RNA in reverse orientation; in vitro-synthesized RNA from this plasmid yielded a negative-strand RNA copy of the MHV DI RNA. When the negative-strand transcripts of the DI RNA were expressed in MHV-infected cells by a vaccinia virus T7 expression system, positive-strand DI RNAs accumulated in the plasmid-transfected cells. DI RNA replication depended on the expression of T7 polymerase and on the presence of the T7 promoter. Transfection of in vitro-synthesized negative-strand transcripts into MHV-infected cells and serial passage of virus samples from RNA-transfected cells also resulted in accumulation of the DI RNA. Positive-strand DI RNA transcripts were undetectable in sample preparations of the in vitro-synthesized negative-strand DI RNA transcripts, and DI RNA did not accumulate after cotransfection of a small amount of positive-strand DI RNA and truncated-replication-disabled negative-strand transcripts; clearly, the DI RNA replicated from the transfected negative-strand transcripts and not from minute amounts of positive-strand DI RNAs that might be envisioned as artifacts of T7 transcription. Sequence analysis of positive-strand DI RNAs in the cells transfected with negative-strand transcripts showed that DI RNAs maintained the DI-specific unique sequences introduced within the leader sequence. These data indicated that positive-strand DI RNA synthesis occurred from introduced negative-strand transcripts in the MHV-infected cells; this demonstration, using MHV, of DI RNA replication from transfected negative-strand DI RNA transcripts is the first such demonstration among all positive-stranded RNA viruses.

Mouse hepatitis virus (MHV), the prototypic coronavirus, contains a single strand of positive-sense RNA that is approximately 31 kb long (3, 25, 26, 39). MHV-infected cells generate seven to eight species of virus-specific mRNAs whose sequences form a 3'-coterminal nested-set structure (23, 27). The mRNAs are numbered 1 to 7 in decreasing order of size (23, 27). MHV particles carry only mRNA 1; only mRNA 1 contains a packaging signal (8). At their 5' ends, all of the mRNAs are fused to a 72- to 77-nucleotide leader sequence (22, 24, 47). MHV mRNA body sequences begin from a transcription consensus sequence of the intergenic region that is located upstream of each gene (22, 24, 35, 47).

Genomic-size and subgenomic-size negative-strand RNAs are present in coronavirus-infected cells in amounts that are significantly smaller than the amounts of corresponding positive-strand RNAs (41, 45). In addition to being template RNAs for genomic replication, the genomic-size negative-strand RNAs may be the template RNAs for transcription of subgenomic mRNAs (2). Subgenomic-size negative-strand RNAs may be template RNAs for subgenomic mRNAs (42–45) or dead-end transcription products (14).

The large size of the coronavirus genome prevents construction of a full-length, infectious cDNA clone. Instead of an infectious cDNA clone, complete cDNA clones of coronavirus

defective interfering (DI) RNAs under the control of the T7 promoter can be used to study coronavirus RNA replication (4, 7, 19–21, 28, 29, 33), transcription (14–18, 32, 50), RNA recombination (38, 51), and RNA packaging (8, 37, 49). Transfection of in vitro-synthesized positive-strand DI RNA transcripts into helper virus-infected cells results in DI RNA replication. Expression of positive-strand DI RNAs by a recombinant T7 vaccinia virus expression system in helper virus-infected cells results in DI RNA replication (29).

Studies with coronavirus DI RNAs have focused on transfecting positive-strand DI RNAs into helper virus-infected cells. Because coronavirus is a positive-strand RNA virus, input positive-strand DI RNAs undergo RNA replication steps that are similar to infectious-virus genomic RNA replication. The presence of significantly larger amounts of positive-strand coronavirus genomic RNAs relative to negative-strand genomic RNAs in infected cells (41, 45) indicates that synthesis of positive-strand genomic RNAs on the negative-strand genomic RNA templates is more efficient than synthesis of negative-strand RNAs on the positive-strand genomic RNA templates. Negative-strand genomic RNAs are potentially excellent templates for RNA replication. In this study, we examined whether introduction of negative-strand MHV DI RNA in MHV-infected cells would result in DI RNA replication and unambiguously showed that DI RNA replicated from the introduced negative-strand DI RNAs.

MATERIALS AND METHODS

Viruses and cells. The plaque-cloned A59 strain of MHV (23) was used as a helper virus. Mouse DBT cells (11) were used for MHV growth and transfection of DNA and RNA. Recombinant vaccinia virus (VV) vTF7-3 that expresses T7

* Corresponding author. Mailing address: Department of Microbiology, The University of Texas at Austin, ESB 304, 24th at Speedway, Austin, TX 78712-1095. Phone: (512) 471-6876. Fax: (512) 471-7088. Electronic mail address: makino@mail.utexas.edu.

[†] Present address: Department of Pathology, Harvard University, Boston, MA 02115.

TABLE 1. Synthetic oligonucleotides used in this study

Oligonucleotide	Sequence
1024	5'-ATCTGATGCATTAAAGTC-3'
1456	5'-ACTACCGAACTGCAATGC-3'
2314	5'-GACACGACGGAAGTGCC-3'
2318	5'-CGACTCACAAGCTTATAAGAGTG-3'
10064	5'-CCAGAGAGACTCGAGAGAAAA-3'
10065	5'-CGTCCTTCTCTAGACCCCGGTCGGCA-3'
10066	5'-TATAAGAGTGATTGGCGTCCG-3'
10079	5'-GTCAGCATGGATATCTTGGTT-3'
10080	5'-GGCAACGCCGTCCTCTTCTTGGGTATCGGC-3'
10106	5'-AGAGAGGGTACGTACGGACGCCATTCACTCTTATAGGGTCGGCATGG-3'
10107	5'-CTTTTCAATATTATTGAAG-3'

RNA polymerase (10) and wild-type VV (WR strain) were grown and subjected to titer determination in RK13 cells.

DNA construction. The synthetic oligonucleotides used in the present study are listed in Table 1. Plasmid pT7ET1 containing both T7 promoter and T7 terminator was constructed by inserting the 0.55-kb *BglII-SspI* fragment of pET17 b (Novagen) into the 2.1-kb *PvuII-SspI* fragment of pT7-4. Insertion of the 2.3-kb *XbaI-HindIII* fragment of DE25 (33) that corresponds to a complete cDNA of DIssE (31, 34) into the large *XbaI-HindIII* fragment of pT7ET1 yielded a plasmid containing negative-strand DIssE cDNA upstream of the T7 terminator; this plasmid contained two T7 promoter sequences. The T7 promoter located close to the T7 terminator was removed by generating a PCR product from DE25 that was primed with oligonucleotide 1456, which has a *StuI* site and binds to 490 to 508 nucleotides from the 5' end of DIssE, and with oligonucleotide 2318, which contains a *HindIII* site and spans the junction of the T7 promoter and the leader sequence of DE25 (33). The 0.5-kb *HindIII-StuI* PCR fragment was inserted into the large *HindIII-StuI* fragment of this plasmid. The pseudoknot ribozyme domain of human hepatitis delta virus (HDV) was then inserted between the leader sequence and the T7 terminator sequence. The HDV ribozyme domain was created by PCR in which the HDV cDNA clone HD489 (30) was incubated with oligonucleotide 10064, which contains a *XhoI* site and binds at nucleotides 792 to 813 of the HDV sequence (30), and oligonucleotide 10065, which contains a *XbaI* site and a *SmaI* site and binds at nucleotides 894 to 921 of the HDV sequence. The *SmaI-XhoI* fragment of the PCR product was then inserted into the *HindIII-XhoI* site of this newly constructed plasmid to yield pDER4. Plasmid pDER4 contains four non-MHV nucleotides (AGCT) between the leader sequence and the ribozyme domain. Consequently, transcripts from pDER4 should have an additional 4 nucleotides at the 3' end. A new PCR product that lacked these 4 nucleotides was made as follows. pDER4 was incubated with oligonucleotide 10106, which contains a *SnaBI* site and binds at the leader, has a part of the HDV ribozyme sequence, and lacks the extra 4 nucleotides, and oligonucleotide 10107, which contains an *SspI* site and binds to pDER4 downstream of the T7 terminator. The 0.45-kb *SnaBI-SspI* PCR fragment was then inserted into the corresponding site of the pDER4, yielding pDER. Purified oligonucleotides were purchased from Integrated DNA Technologies, Coralville, Iowa. For each mutant, we sequenced the region of the insertion obtained by PCR.

DNA transfection. DBT cells were infected with vTF7-3 or wild-type VV at a multiplicity of infection of 5. At 1.5 h postinfection (p.i.), DBT cells were transfected with 10 µg of DNA by lipofection as specified by the manufacturer (Gibco BRL). At 6 h after VV infection, cells were infected with MHV at a multiplicity of infection of 5. After adsorption of MHV for 1 h, the cells were incubated with a medium containing 40 µg of cytosine-β-D-arabinofuranoside (ara-C) (Sigma) per ml to suppress VV DNA replication.

RNA transcription and transfection. Plasmid DNAs were linearized with appropriate restriction enzymes, and capped RNAs were transcribed with T7 RNA polymerase by using mMESSAGEmMACHINE T7 kit (Ambion) as specified by the manufacturer. MHV-infected DBT cells were transfected with in vitro-synthesized RNA at 1 h p.i. by a lipofection procedure, as previously described (32).

Preparation of virus-specific intracellular RNA. Viral RNAs in virus-infected cells were extracted as previously described (36). In some experiments, RNA samples were treated with RNase-free DNase I (Promega) and *MspI* at 37°C for 4 h.

Northern blotting. Northern (RNA) blot analysis with a random-primed probe corresponding to the 0.55-kb *SstI-SphI* fragment of DE25 was performed as previously described (14). For detection of positive-stranded MHV RNA, 5'-end-labeled oligonucleotide 10080, which binds at nucleotides 931 to 960 of DE25 from the 5' end, was used as a probe.

RT-PCR. Positive-strand DI RNA specific-cDNAs were synthesized by incubating intracellular RNA species with oligonucleotide 10079, which binds to positive-strand DI RNA at nucleotides 892 to 912 from the 5' end, as described previously (34); this oligonucleotide binds about 3 kb from the 5' end of helper virus genomic RNA (34). After cDNA synthesis, reverse transcriptase (RT) was

inactivated by incubating the sample at 95°C for 10 min and free oligonucleotides were removed by spin column chromatography on Sephadex G-50. The RT-PCR products were synthesized after incubating cDNAs with oligonucleotide 10066, which binds to the 5' end of leader sequence, and oligonucleotide 1024, which binds at the junction site of domains I and II of positive-strand DIssE (34). PCR was carried out for 30 cycles of 94°C for 1 min, 57°C for 1 min, and 72°C for 1 min.

Sequence analysis. The gel-purified RT-PCR products were sequenced by the direct PCR sequencing procedure established by Winship (54). Further analysis of RT-PCR products was carried out by cloning RT-PCR products into a TA cloning vector (Invitrogen).

RESULTS

MHV DI RNA replication after recombinant VV-mediated expression of negative-strand DI RNA transcripts in MHV-infected cells. We constructed two plasmids, pDER and pDER4, to study whether negative-strand transcripts of MHV DI RNA could initiate DI RNA replication. A complete cDNA of MHV DI RNA, DIssE, was inserted between the T7 promoter and the HDV ribozyme domain in both plasmids, and the T7 terminator was inserted downstream of the ribozyme domain to further ensure termination; T7 polymerase-mediated transcripts from these constructs yielded negative-strand copies of DIssE (Fig. 1). The 5' ends of the transcripts were expected to contain short stretches of non-MHV sequences derived from part of the T7 promoter and a plasmid polylinker site; the DI RNA sequence, which contained a poly(U) sequence at the 5'-end region, and a sequence complementary to the leader sequence (antileader) at the 3' end followed these non-MHV sequences. The leader sequence of pDER and pDER4 had five substituted nucleotides relative to the MHV leader sequence (Fig. 1B). Furthermore, the leader sequence of pDER and pDER4 had four repeats of UCUAA at the junction of the leader and body sequences and lacked the 9-nucleotide sequence (UUUAUAAAC) downstream of the UCUAA repeats (on the positive strand) while MHV had two UCUAA repeats and contained the 9-nucleotide sequence (33) (Fig. 1B). In addition, pDER4 had an extra 4 nucleotides, AGCT, between the 3' end of the leader sequence and the ribozyme domain; negative-strand transcripts of pDER4 should have the corresponding (UCGA) additional non-MHV sequence at the 3' end. We used these extra nucleotides for examining de novo initiation of positive-strand DI RNA synthesis (see below).

We examined whether recombinant VV-mediated expression of negative-strand transcripts of pDER and pDER4 resulted in DI RNA replication in MHV-infected cells. Each plasmid DNA was transfected into the vTF7-3-infected DBT cells, and at 6 h p.i., the cells were infected with MHV. We extracted intracellular RNA 12 h after MHV infection and selected poly(A)-containing RNAs by oligo(dT) column chromatography (31). We hybridized Northern blots with 5'-end-labeled oligonucleotide 10080 as a probe for positive-strand DI

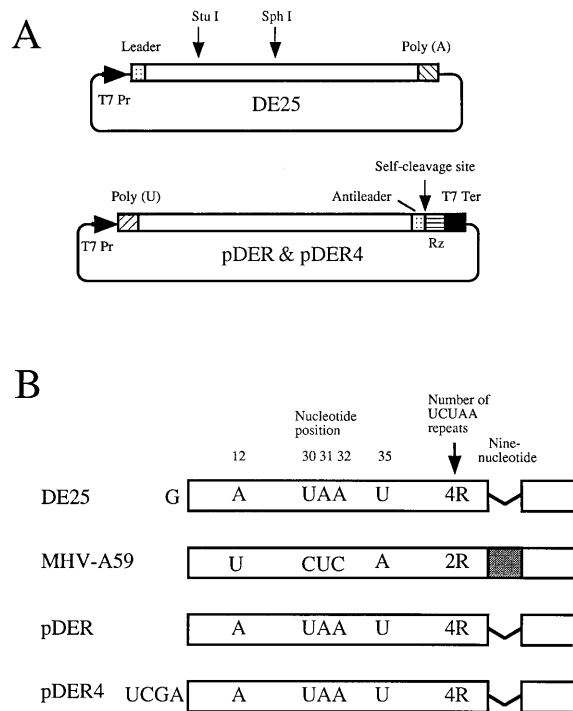


FIG. 1. Schematic representation of the transcription plasmids (A) and diagram of the 5'-end sequences of the DI RNA transcripts in the positive sense (B). (A) Plasmid DE25 encodes positive-strand MHV DIssE RNA, and plasmids pDER and pDER4 encode the negative-strand MHV DIssE RNA. T7 Pr, bacteriophage T7 promoter site; Rz, ribozyme from HDV; T7 Ter, T7 transcription terminator. (B) DE25 and MHV represent the 5'-end sequence of DE25 transcripts and MHV genomic RNA, respectively. The diagram of pDER and pDER4 represents complementary sequences of the 3' end of the transcripts of these plasmids. The nucleotide sequences which are not denoted share the same sequence as described previously (33). 2R and 4R represent two and four repeats of UCUGA sequence, respectively. The shaded box represents the 9-nucleotide (UUUUAAAAC) sequence in MHV. The 9-nucleotide sequence that is deleted is shown as a thin line. The G nucleotide at the 5' end of DE25 represents an extra nucleotide present in DE25 transcripts (33). Similarly, UCGA nucleotides in pDER4 represent extra nucleotides present in the initial transcripts in pDER4. Because initial transcripts of pDER4 are negative sense, the extra nucleotides at the 3' end of pDER4 transcripts should be 5'-UCGA-3'.

RNA synthesis; this probe hybridizes with only positive-strand DI RNAs and MHV mRNA 1 (Fig. 2A). Positive-strand DI RNAs accumulated in the plasmid-transfected, vTF7-3, MHV-infected cells, but not in MHV-uninfected cells, suggesting that positive-strand DI RNAs were synthesized from the vTF7-3-mediated negative-strand DI RNA transcripts by MHV replication machinery. We frequently observed broad RNA signals that migrated much more slowly than DIssE RNA (Fig. 2A); these signals most probably represented helper virus-derived DI RNAs.

To confirm that the positive-strand DI RNA in the DNA-transfected cells was accumulating as a result of replication, we examined DI RNA replication in the cells infected with passaged virus samples. The culture fluid was harvested from plasmid-transfected cells 16 h after infection with MHV, and cell debris was removed by low-speed centrifugation. This sample, the passage 0 virus sample, was used for inoculating fresh DBT cells to obtain the passage 1 virus sample. To inhibit recombinant VV DNA replication and recombinant VV-mediated transcription from contaminated plasmid DNA in the inoculum, ara-C and 2.5 μ g of actinomycin D per ml were added to the culture media and passage 1 virus was harvested

at 16 h p.i. We prepared passage 2 virus sample by the same procedure as for passage 1 virus. DBT cells were infected with passage 0 virus sample and incubated with actinomycin D and ara-C. Intracellular RNA was extracted at 7 h p.i., and DI RNA replication was examined by Northern blot analysis with a random-primed probe that hybridizes with only DI RNA and MHV mRNA 1 (Fig. 2B). DI RNAs replicated efficiently in the cells infected with passage 0 virus samples from DNA-transfected, MHV-infected cells that were infected with vTF7-3. The majority of detected DI RNAs were positive-strand DI RNAs, because most of these DI RNAs bound to oligo(dT) cellulose (data not shown). Negative-strand DI RNAs were underdetectable by Northern blot analysis with an oligonucleotide probe that specifically hybridized to negative-strand DI RNA, yet the presence of negative-strand DI RNAs was confirmed by RT-PCR in which the initial cDNA was synthesized from negative-strand DI RNAs (data not shown). These data demonstrated that DI RNA replicated in the presence of MHV and suggested the possibility that DI RNA replicates from the negative-strand DI RNA transcripts.

Dependency of DI RNA replication on expression of T7 polymerase and the presence of the T7 promoter in the plasmid. To confirm that DI RNA replicated exclusively from DI RNA negative-strand transcripts that were expressed by T7 polymerase, we tested the possibility that an unidentified VV gene product(s) synthesizes positive-strand DI RNA transcripts from the transfected plasmid; we studied whether DI RNA replicated in the wild-type VV-infected cells. DBT cells were infected with wild-type VV and then transfected with

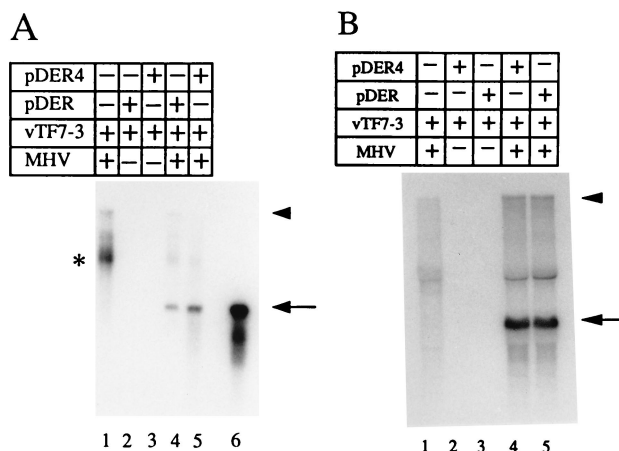


FIG. 2. Replication of DI RNAs in plasmid-transfected cells (A) and passage 0 virus-infected cells (B). (A) Recombinant VV, vTF7-3 infected DBT cells were mock transfected (lane 1) or transfected with pDER (lanes 2 and 4), or pDER4 (lanes 3 and 5). At 6 h p.i., the cells were infected with MHV (lanes 1, 4, and 5) or mock infected (lanes 2 and 3). Intracellular RNA was extracted 12 h after MHV infection. Poly(A)-containing RNAs were collected, separated by 1% formaldehyde gel electrophoresis, and transferred to a nylon membrane. The 5'-end-labeled oligonucleotide 10080 that hybridizes with positive-strand DI RNA and MHV mRNA 1 was used as a probe. Lane 6 represents in vitro-synthesized DE25 DI RNA. The arrowhead and arrow indicate MHV mRNA 1 and DI RNA, respectively. The asterisk most probably represents helper virus-derived DI RNAs. (B) Recombinant VV-infected DBT cells were mock transfected (lane 1), or transfected with pDER (lanes 3 and 5), or pDER4 (lanes 2 and 4). At 6 h after vTF7-3 infection, the cells were infected with MHV (lanes 1, 4, and 5) or mock infected (lanes 2 and 3). Passage 0 virus samples were harvested 16 h after MHV infection and then inoculated into fresh DBT cells. Intracellular RNAs were extracted at 7 h from passage 0 virus-infected cells, separated by 1% formaldehyde gel electrophoresis, and transferred to a nylon membrane. The probe was prepared by random-primed 32 P labeling of the MHV DI cDNA small *Stu*I-*Sph*I fragment (Fig. 1A); it hybridizes with DI RNA and MHV mRNA 1. The arrowhead and arrow indicate MHV mRNA 1 and DI RNA, respectively.

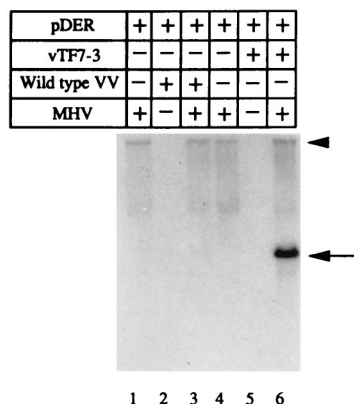


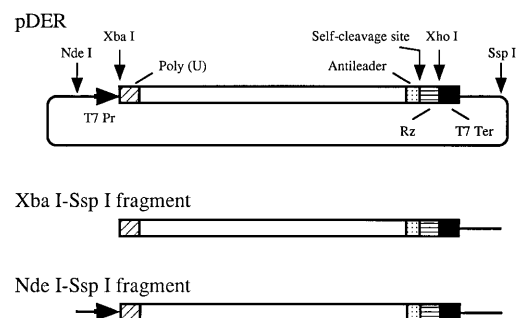
FIG. 3. Requirement of T7 polymerase expression for DI RNA replication. DBT cells were infected with wild-type VV (lanes 2 and 3) or vTF7-3 (lanes 5 and 6). VV-infected cells were then transfected with pDER. At 6 h after VV infection, the cells were infected with MHV (lanes 1, 3, 4, and 6) or mock infected (lanes 2 and 5). Intracellular RNAs were extracted from passage 0 virus-infected cells and analyzed by Northern blotting. The arrowhead and arrow indicate MHV mRNA 1 and DI RNA, respectively.

pDER plasmid DNA. As a control, we used vTF7-3. After 6 h of VV infection, the cells were mock infected or infected with MHV, and passage 0 virus samples were collected. Northern blot analysis showed that for passage 0 virus-infected cells in the presence of actinomycin D and ara-C, DI RNA replicated in cells infected with vTF7-3 but not in those infected with wild-type VV (Fig. 3), demonstrating that DI RNA replication exclusively required expression of T7 polymerase in the DNA-transfected cells.

Next, we ruled out the possibility that T7 polymerase recognizes an unidentified cryptic promoter(s) on the plasmid, thereby synthesizing positive-strand DI RNA transcripts; we studied whether DI RNA replication depended only on the presence of the T7 promoter and not on another cryptic promoter for T7 polymerase. We used two restriction fragments, the *Nde*I-*Ssp*I fragment and the *Xba*I-*Ssp*I fragment (Fig. 4A). The *Nde*I-*Ssp*I fragment consisted of the following domains from the 5' to 3' direction: a 0.3-kb plasmid sequence upstream of the T7 promoter, the T7 promoter, an entire DI cDNA, the ribozyme domain, the T7 terminator, and a 0.5-kb plasmid sequence located downstream of the T7 terminator. The *Xba*I-*Ssp*I fragment had a similar structure, except that it lacked all the sequences upstream of the poly(U) sequence, including the T7 promoter. DI RNA replication occurring after transfection of the *Nde*I-*Ssp*I fragment but not after transfection of the *Xba*I-*Ssp*I fragment would demonstrate that a putative cryptic promoter for positive-strand DI RNA transcription did not exist between the T7 terminator and the *Ssp*I site and that the DI RNA replicated from the negative-strand DI RNA transcripts that were transcribed from the T7 promoter. Passage 1 virus samples were obtained from cells that were independently transfected with equal amounts of a gel-purified *Xba*I-*Ssp*I fragment and an *Nde*I-*Ssp*I fragment. Northern blot analysis of intracellular RNA from passage 1 virus-infected cells showed that DI RNA replicated after transfection of the *Nde*I-*Ssp*I fragment but not after transfection of the *Xba*I-*Ssp*I fragment (Fig. 4B). This result demonstrated that putative positive-strand DI RNA transcription from a cryptic promoter for T7 polymerase did not happen after transfection of the *Xba*I-*Ssp*I fragment. DI RNA replication depended on the presence of the T7 promoter, indicating that DI RNA replicated from expressed negative-strand transcripts.

DI RNA replication initiated from the transfected in vitro-synthesized negative-strand DI RNA transcripts. The data strongly suggested that DI RNA replicated from the expressed negative-strand transcripts. However, we could not completely eliminate the possibility that positive-strand DI RNAs are synthesized by unusual mechanisms in vTF7-3-infected cells; e.g., T7 RNA polymerase might jump to the complementary DNA template strand at the 3' end and begin copying. To address this possibility, we examined whether DI RNA could replicate from in vitro-synthesized negative-strand DI RNA transcripts that were transfected into MHV-infected cells. Plasmids pDER and pDER4 were linearized by restriction digestion with *Xho*I (Fig. 4A), and RNA was synthesized in vitro. MHV-infected DBT cells were independently transfected with 40 μ g of in vitro-synthesized pDER and pDER4 transcripts. At 16 h p.i., passage 0 virus sample was harvested and further passed to obtain passage 1 and 2 viruses. Northern blot analysis of intracellular RNAs showed accumulation of DI RNAs of the expected size in passage 1 and 2 virus-infected cells (Fig. 5). In most cases, after RNA transfection, DI RNAs became apparent in passage 1 virus-infected cells and were not seen in passage 0 virus-infected cells, showing that DI RNAs accumulated less efficiently from the transfected negative-strand RNA transcripts than from the plasmid-transfected cells (Fig. 2 and

A



B

Xba I-Ssp I	-	-	+	-
Nde I-Ssp I	-	-	-	+
vTF7-3	-	+	+	+
MHV	+	+	+	+

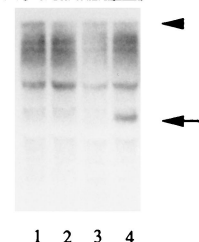


FIG. 4. Requirement of T7 promoter sequence for DI RNA replication. (A) Schematic representation of pDER and its *Xba*I-*Ssp*I and *Nde*I-*Ssp*I fragments. (B) Northern blot analysis of intracellular DI RNAs. Mock-infected DBT cells (lane 1) or vTF7-3-infected DBT cells (lanes 2 to 4) were mock transfected (lanes 1 and 2) or transfected with the pDER *Xba*I-*Ssp*I fragment (lane 3) or the pDER *Nde*I-*Ssp*I fragment (lane 4). At 6 h after VV infection, cells were infected with MHV. Intracellular RNAs extracted from passage 1 virus-infected cells were analyzed by Northern blot analysis. The arrowhead and arrow indicate MHV mRNA 1 and DI RNA, respectively.

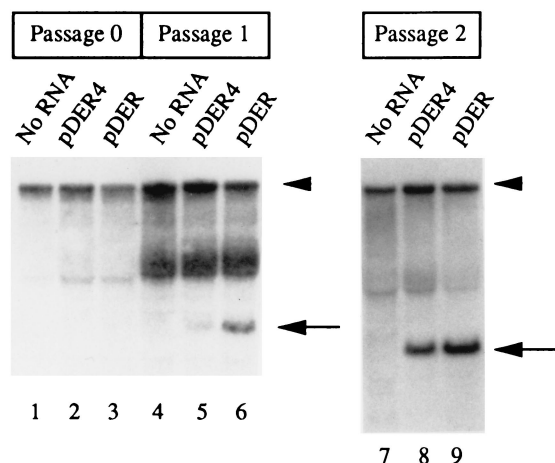


FIG. 5. DI RNA replication after transfection of in vitro-synthesized negative-strand DI RNA transcripts. MHV-infected DBT cells were mock transfected (lanes 1, 4, and 7) or transfected with in vitro-synthesized pDER4 transcripts (lanes 2, 5, and 8) or in vitro-synthesized pDER transcripts (lanes 3, 6, and 9). Intracellular RNAs were extracted from passage 0 virus-infected cells (lanes 1 to 3), passage 1 virus-infected cells (lanes 4 to 6), or passage 2 virus-infected cells (lanes 7 to 9) and analyzed by Northern blot. The arrowhead and arrow indicate MHV mRNA 1 and DI RNA, respectively.

5). This difference probably reflected the amount of negative-strand DI RNA transcripts in the cells; many of the transfected negative-strand DI RNA transcripts probably did not enter the cytoplasm and/or were rapidly degraded, whereas vTF7-3-mediated negative-strand DI RNA transcripts were continuously produced in large quantities in the cytoplasm (data not shown).

We wanted to rule out the possibility that DI RNA was replicating from contaminating positive-strand RNAs in our negative-strand DI RNA preparation. By using Northern blot analysis with an oligonucleotide probe that specifically hybridizes to the positive-strand DI RNA, we searched for putative positive-strand DI RNA transcripts in the in vitro-synthesized pDER RNA preparation (Fig. 6). In vitro-synthesized positive-strand DIssE RNA, DE25 (33) (Fig. 1), was the positive control. We detected positive-strand DE25 transcripts in samples diluted 10^2 - to 10^4 -fold, whereas we could not detect any positive-strand DI RNAs in the undiluted in vitro-synthesized pDER RNA preparation (Fig. 6). These data suggested that in vitro-synthesized pDER transcripts did not contain positive-strand DI RNAs or that the level of positive-strand DI RNAs in the transcripts was so minute as to be undetectable.

Although positive-strand transcripts were not detectable by Northern blot analysis, we could not completely rule out the possibility that DI RNA replicated from a minute amount of possible contaminating positive-strand DI RNA transcripts. To address this possibility, we determined whether DI RNA replicated after cotransfection of a small amount of added positive-strand DE25 DI RNA along with a truncated, disabled negative-strand pDER RNA. Truncated pDER negative-strand RNA transcripts were synthesized after digestion of pDER with *Stu*I (Fig. 7A); these transcripts lacked the 3'-end 0.45 kb of the pDER negative strand. The 0.45-kb region is part of the DIssE *cis*-acting replication signal (19); consequently, DI RNA should not replicate from the negative-strand transcripts of the truncated pDER. For the mixed transfection experiment into MHV-infected cells, we transfected truncated pDER negative-strand RNA transcripts along with a 100-fold dilution of DE25 positive-strand transcripts (approximately 3×10^{11} molecules) (10^{-2} and 10^{-4} dilutions of DE25 are shown in Fig. 6). This

amount of positive-strand transcripts was at least 100 times more abundant than any putative positive-strand DI RNA transcripts present in the in vitro-synthesized pDER transcript preparation, as shown in Fig. 6. In vitro-synthesized pDER negative-strand transcripts served as a control in a parallel transfection, with the amount of control RNA being equivalent to the combined amounts of the RNAs in the mixed experimental transfection. After serial passage, analysis of intracellular RNAs from cells infected with passage 2 virus showed that DI RNA accumulated efficiently in the cells infected with virus harvested from pDER-transfected control cells but not in the cells infected with virus harvested from the cotransfected cells (Fig. 7B). If DI RNA was replicating from trace amounts of contaminating positive-strand RNAs in pDER in vitro-synthesized RNA preparations, we should have seen DI RNA accumulating in the cells that were cotransfected with positive-strand and disabled truncated-negative strand. Clearly, MHV DI RNA replicated from only the negative-strand transcripts of pDER.

Characterization of the leader sequence of replicating DI RNAs. The de novo initiation of positive-strand DI RNA synthesis from the introduced negative-strand DI RNA transcripts was tested by analyzing the leader sequence of positive-strand DI RNAs obtained from pDER4-transfected cells. The leader sequence of pDER4 differed from that of the helper virus: the pDER4 leader sequence incorporated an additional 4 nucleotides at the 3' end of its in vitro transcripts, four UCUAA repeats, and five nucleotide substitutions, while it lacked a unique 9-nucleotide sequence (Fig. 1B). These differences helped identify whether synthesis of positive-strand RNA was initiated in the pDER4-transfected cells. If positive-strand DI RNA synthesis initiates from the 3' end of the negative-strand transcripts, the first positive-strand DI RNAs that are made should have a leader sequence that is an exact copy of the pDER4 antileader sequence. If positive-strand DI RNA initiates from the positive-strand genomic leader sequence that is derived from helper virus (33), the entire leader sequence of pDER4 should change to that of the helper virus. These speculations were based on our previous observation that soon

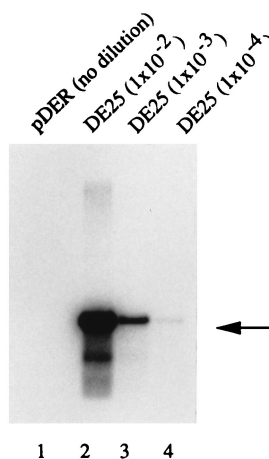


FIG. 6. Positive-strand transcripts in the preparation of in vitro-synthesized pDER transcripts. The in vitro-synthesized RNAs were prepared from the same amount of pDER plasmid and DE25 plasmid. Undiluted transcripts from pDER (lane 1), 100-fold-diluted DE25 transcripts (lane 2), 1,000-fold-diluted DE25 transcripts (lane 3), or 10,000-fold-diluted DE25 transcripts were subjected to 1% formaldehyde agarose gel electrophoresis. Northern blot analysis was performed with an oligonucleotide probe which specifically hybridizes with positive-strand but not negative-strand DI RNAs. The arrow indicates DE25 transcripts of the expected size.

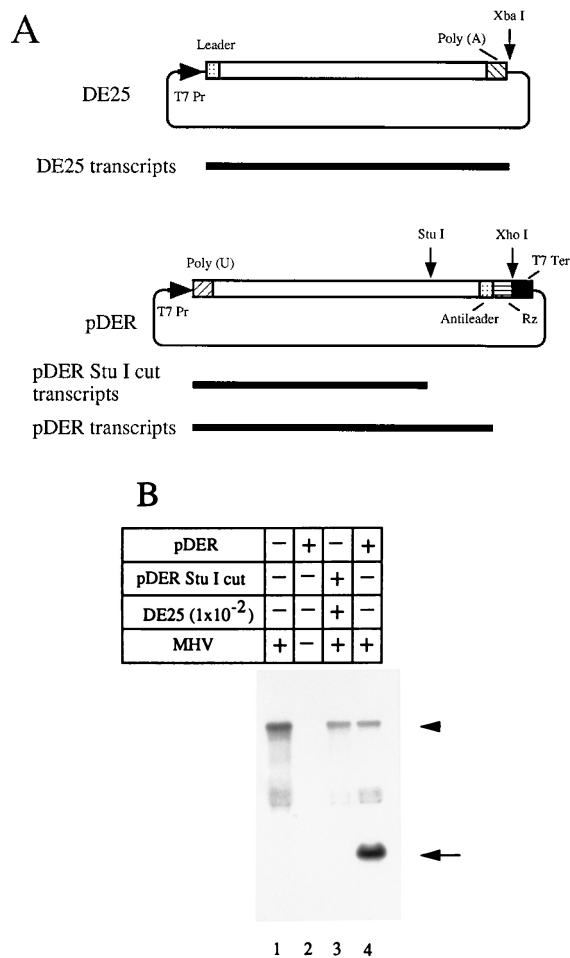


FIG. 7. Evidence that DI RNA replicated from the negative-strand pDER transcripts but not from positive-strand transcripts possibly present in the preparation of pDER negative-strand transcripts. (A) Schematic representation of DE25 plasmid, DE25 positive-sense transcripts, pDER plasmid, pDER negative-sense transcripts, and truncated pDER negative-sense transcripts. (B) Northern blot analysis of intracellular DI RNAs. Mock-infected DBT cells (lane 2) or MHV-infected DBT cells (lanes 1, 3, and 4) were mock transfected (lane 1), transfected with in vitro-synthesized pDER transcripts (lanes 2 and 4), or transfected with a mixture of 100-fold-diluted DE25 in vitro-synthesized transcripts and in vitro-synthesized transcripts from the *Stu*I-digested pDER4. The total amount of RNAs used for transfection in lanes 2, 3, and 4 was the same. Intracellular RNAs extracted from passage 2 virus-infected cells were analyzed by Northern blot analysis with random-primed 32 P-labeling of the MHV DI cDNA small *Stu*I-*Sph*I fragment (Fig. 1A). The arrowhead and arrow indicate MHV mRNA 1 and DI RNA, respectively.

after transfection of positive-strand DI RNAs into MHV-infected cells, entire leader sequences of DI RNAs switch to helper-virus leader sequences (33). Because multiple cycles of DI RNA replication probably would select a specific type of DI RNA that replicates well under given conditions, we attempted to characterize positive-strand DI RNAs early after introduction of the negative-strand transcripts. We characterized positive-strand DI RNAs in cells transfected with pDER4 transcripts by sequencing positive-strand DI RNA-specific RT-PCR product. The negative-strand pDER4 transcripts were prepared in vitro, extensively treated with RNase-free DNase I and *Msp*I, and transfected into MHV-infected cells. Intracellular viral RNA was extracted from RNA-transfected cells at 8 h after MHV infection and incubated with DNase I. We amplified the 5' region of positive-strand DI RNAs by RT-

PCR as described in Materials and Methods. We detected the expected RT-PCR product from RNA-transfected, MHV-infected cells, whereas we did not detect this product in the RNA-transfected, mock-infected cells or in mock-transfected, MHV-infected cells (data not shown), indicating that the RT-PCR product was indeed derived from positive-strand DI RNAs. Then the PCR product was purified on an agarose gel and cloned into a plasmid vector. Sequencing analysis of eight clones showed that all of the cloned RT-PCR products contained DI-specific leader sequence. One sequence analysis is shown in Fig. 8A. A nucleotide substitution at nucleotide 12 (Fig. 1B) was not detectable by this analysis, because the oligonucleotide used for RT-PCR included this region. To further confirm that the RT-PCR product was not derived from contaminated plasmid DNA but from positive-strand DI RNAs, we extracted intracellular RNAs from passage 0 virus sample-infected cells and carried out RT-PCR to amplify the positive-strand DI RNA leader sequence. Direct sequencing of the RT-PCR product showed that the leader sequence derived from pDER4 maintained its DI-specific sequence (Fig. 8B). These data showed that the leader sequence of the positive-strand DI RNA did not contain helper virus genomic leader sequence but contained a sequence that was complementary to the leader sequence of pDER4 transcripts.

We examined whether the extra 4 nucleotides at the 3' end of the transcripts were maintained in the positive-strand DI RNA. Although we used many different procedures that would identify the 5' end of positive-strand DI RNAs (5, 9, 13, 53), all these PCR-based procedures failed to work in our hands (data not shown). As an alternative approach, we characterized positive-strand DI RNA by primer extension. Passage 0 virus sample was prepared from pDER4 plasmid DNA-transfected cells, and intracellular RNAs were extracted from passage 0 virus-

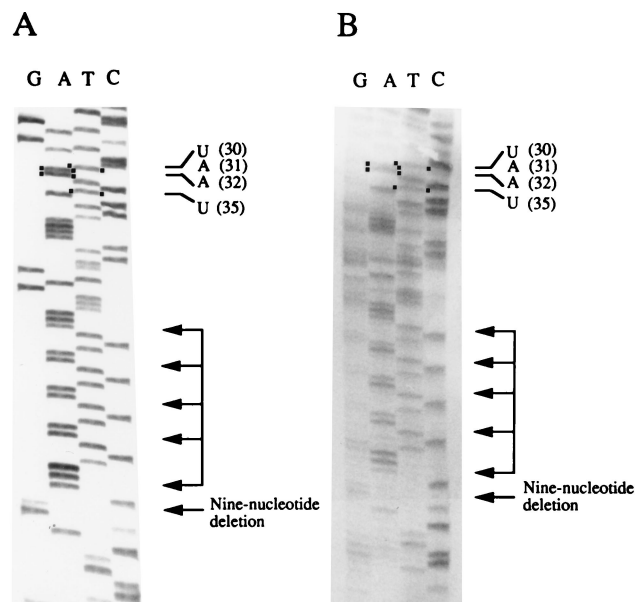


FIG. 8. Leader sequence of positive-strand DI RNAs that were synthesized after transfection of in vitro-synthesized pDER4 RNA transcripts. The UCUAA repeats are shown by arrows. The unique nucleotides that are specific for pDER4 DI RNA are also shown. Numbers in the parentheses are nucleotide positions from the 5' end of the positive-strand DI RNA (Fig. 1B). (A) Sequence of leader region of cloned RT-PCR product of positive-strand DI RNAs isolated from cells transfected with pDER4 transcripts. (B) Direct sequencing analysis of the RT-PCR product of positive-strand pDER4 DI RNAs isolated from passage 0 virus-infected cells.

infected cells. Primer extension analysis with 5'-end-labeled oligonucleotide 2314 that binds to positive-strand DI RNAs at 82 to 98 nucleotides from the 5' end showed that most of the primer extension product comigrated with DE25 DI RNA (data not shown); we did not detect a primer extension product that had an extra 4 nucleotides. These data indicated that DI RNAs with the extra 4 nucleotides did not accumulate in passage 0 virus-infected cells. Because other unique DI RNA-specific sequences present in the leader sequence of pDER4 were maintained in the positive-strand DI RNA, positive-strand DI RNA synthesis probably initiated from the introduced negative-strand DI RNA transcripts.

DISCUSSION

We have demonstrated that VV T7-mediated expression of negative-strand DI RNAs in MHV-infected cells resulted in MHV DI RNA replication. DI RNA replicated only when vTF7-3 but not wild-type VV was used, demonstrating that template RNAs for DI RNA replication were synthesized by the T7 polymerase-mediated mechanism. We also showed that DI RNA replication required the T7 promoter sequence on the plasmid, demonstrating that initial transcripts used for positive-strand DI RNA synthesis were transcribed from the T7 promoter, i.e., negative-strand DI RNA transcripts. These data strongly suggested that DI RNA replicated from the expressed negative-strand DI RNA transcripts.

MHV DI RNA also replicated after transfection of in vitro-synthesized negative-strand DI RNA transcripts in MHV-infected cells. We did not detect positive-strand DI RNA transcripts in the in vitro transcripts by Northern blot analysis. Furthermore, DI RNA did not replicate after cotransfection of truncated negative-strand DI RNA transcripts and in vitro-synthesized positive-strand DI RNA transcripts that were at least 100 times more abundant than the putative positive-strand DI RNAs that might have been present in the in vitro-synthesized negative-strand transcripts. These studies eliminated the possibility that putative positive-strand DI RNA transcripts in the preparation of negative-strand RNA transcripts initiated DI RNA replication. DI RNA indeed replicated from the transfected negative-strand DI RNA transcripts.

Characterization of the leader sequence of replicating DI RNA showed that DI RNAs contained the DI-specific leader sequence, suggesting that positive-strand DI RNAs initiated from the transfected negative-strand DI RNA transcripts. However, we did not have direct evidence of *de novo* initiation of positive-strand DI RNA from the input negative-strand transcripts, because we could not detect positive-strand DI RNA molecules that retained the extra 4 nucleotides at the 5' end. One explanation for how the extra sequence at the 5' end of positive-strand DI RNAs was lost is that the MHV RNA polymerase may have selected the correct initiation site for positive-strand synthesis from within the negative-strand template. Alternatively, DI RNAs lacking the extra nucleotides may have been generated during replication of DI RNAs and may have replicated much more efficiently than DI RNAs containing the extra nucleotides. Trimming of the 3'-end extra nucleotides at the expressed negative-strand MHV DI RNA transcripts may not be specific for MHV DI RNAs; extra nucleotides at the 5' end of in vitro-synthesized positive-strand poliovirus RNA are removed during poliovirus RNA replication (52), and extra nucleotides at the 3' end of expressed negative-strand RNA 2 of flock house virus are also trimmed during accumulation of positive-stranded RNA 2 (1).

Only a few other examples of positive-strand RNA synthesis

from input negative-strand RNAs of positive-strand RNA viruses exist. These include MS2 RNA phage (46), satellite RNA of cucumber mosaic virus (48), and the RNA 2 fragment of flock house virus (1). Another example was shown in the coronavirus transmissible gastroenteritis virus; noncoronavirus RNAs containing the negative-sense transcription consensus sequence of transmissible gastroenteritis virus also serve as templates for transcription in transmissible gastroenteritis virus-infected cells (12). These studies, however, did not rigorously eliminate the possibility that RNA synthesis started from a minute amount of positive-strand RNA transcripts that might have been present in transfected RNA preparations or that might have been synthesized spuriously from the transfected DNA by T7 polymerase. To our knowledge, for all positive-strand RNA viruses, the data presented here provide the first example of DI RNA replication resulting from input negative-strand DI RNA transcripts. The DI RNAs used in this study do not require a DI RNA-specific protein for DI RNA replication (28); as a result, the *trans*-acting factors provided by helper virus and host cells sufficiently drive DI RNA replication. In this regard, the prerequisites for MHV DI RNA replication seem to be different from those for poliovirus RNA synthesis, in which a virus-specific protein seems to function only in *cis* for initiation of virus RNA synthesis (6).

The amount of coronavirus genomic-size negative-strand RNA is much smaller than that of positive-strand genomic size RNAs (45). This suggests that negative-strand RNAs are much more efficient templates. Transfection of in vitro-synthesized positive-strand DI RNA transcripts into MHV-infected cells results in immediate accumulation of DI RNA within RNA-transfected cells (33). We found that detectable levels of DI RNA accumulated only after serial passage of virus samples from cells transfected with negative-strand transcripts (Fig. 5). The amount of the transfected negative-strand DI RNAs was significantly larger than that of the negative-strand DI RNAs found in DI RNA replicating cells. Thus, negative-strand DI RNAs that were transfected into MHV-infected cells were poor template RNAs for positive-strand DI RNA synthesis. Probably, RNA replicates more efficiently when the template RNAs are double-stranded RNAs. Two lines of evidence support this hypothesis: most negative-strand MHV RNAs seem to be present as double-stranded RNAs (41), and at least one region of positive-strand DI RNA is necessary for positive-strand DI RNA synthesis. Synthesis of positive-strand DI RNA requires a region of about 60 nucleotides located in the middle of MHV DI RNA (21). We saw that in this region, the RNA secondary structure of the positive strand but not the negative strand was important for biological function (40). Positive-strand RNA synthesis did not occur efficiently in the absence of the part of the positive-strand RNA that is associated with negative-strand transcripts. This may be one of the reasons why the negative-strand RNAs synthesized in MHV-infected cells, which probably associate with the 60-nt long positive-strand DI RNA region to form double-stranded RNA, are excellent templates for positive-strand RNA synthesis whereas transfected negative-strand RNA templates, which probably exist as single-stranded RNAs, are less effective templates.

ACKNOWLEDGMENTS

We thank Bernard Moss, National Institutes of Health, for vTF7-3 and wild-type VV. We also thank Stephen Stohlman, Susan Baker, and Brenda Hogue for valuable advice on the use of vaccinia viruses.

This work was supported by Public Health Service grants AI29984 and AI32591 from the National Institutes of Health.

REFERENCES

- Ball, L. A. 1994. Replication of the genomic RNA of a positive-strand RNA animal virus from negative-sense transcripts. *Proc. Natl. Acad. Sci. USA* **91**:12443–12447.
- Baric, R. S., S. A. Stohlman, and M. M. C. Lai. 1983. Characterization of replicative intermediate RNA of mouse hepatitis virus: presence of leader RNA sequences on nascent chains. *J. Virol.* **48**:633–640.
- Bonilla, P. J., A. E. Gorbalenya, and S. R. Weiss. 1994. Mouse hepatitis virus strain A59 RNA polymerase gene ORF 1a: heterogeneity among MHV strains. *Virology* **198**:736–740.
- Chang, R.-Y., M. A. Hofmann, P. B. Sethna, and D. A. Brian. 1994. A *cis*-acting function for the coronavirus leader in defective interfering RNA replication. *J. Virol.* **68**:8223–8231.
- Chen, Z., K. S. Faaberg, and P. G. W. Plagemann. 1994. Determination of the 5' end of the lactate dehydrogenase-elevating virus genome by two independent approaches. *J. Gen. Virol.* **75**:925–930.
- Collis, P. S., B. J. O'Donnell, D. J. Barton, J. A. Rogers, and J. B. Flanagan. 1992. Replication of poliovirus RNA and subgenomic RNA transcripts in transfected cells. *J. Virol.* **66**:6480–6488.
- de Groot, R. J., R. G. van der Most, and W. J. M. Spaan. 1992. The fitness of defective interfering murine coronavirus DI-a and its derivatives is decreased by nonsense and frameshift mutations. *J. Virol.* **66**:5898–5905.
- Fosmire, J. A., K. Hwang, and S. Makino. 1992. Identification and characterization of a coronavirus packaging signal. *J. Virol.* **66**:3522–3530.
- Frohman, M. A., M. K. Dush, and G. R. Martin. 1988. Rapid production of full-length cDNAs from rare transcripts: amplification using a single gene-specific oligonucleotide primer. *Proc. Natl. Acad. Sci. USA* **85**:8998–9002.
- Fuerst, T. R., E. G. Niles, F. W. Studier, and B. Moss. 1986. Eukaryotic transient-expression system based on recombinant vaccinia virus that synthesizes bacteriophage T7 RNA polymerase. *Proc. Natl. Acad. Sci. USA* **83**:8122–8126.
- Hirano, N., K. Fujiwara, S. Hino, and M. Matsumoto. 1974. Replication and plaque formation of mouse hepatitis virus (MHV-2) in mouse cell line DBT culture. *Arch. Gesamte Virusforsch.* **44**:298–302.
- Hiscox, J. A., K. L. Mawditt, D. Cavanagh, and P. Britton. 1995. Investigation of the control of coronavirus subgenomic mRNA transcription by using T7-generated negative-sense RNA transcripts. *J. Virol.* **69**:6219–6227.
- Hofmann, M. A., and D. A. Brian. 1991. A PCR-enhanced method for determining the 5' end sequences of mRNAs. *PCR Methods Appl.* **1**:43–45.
- Jeong, Y. S., and S. Makino. 1992. Mechanism of coronavirus transcription: duration of primary transcription initiation activity and effect of subgenomic RNA transcription on RNA replication. *J. Virol.* **66**:3339–3346.
- Jeong, Y. S., and S. Makino. 1994. Evidence for coronavirus discontinuous transcription. *J. Virol.* **68**:2615–2623.
- Jeong, Y. S., J. F. Repass, Y.-N. Kim, S. M. Hwang, and S. Makino. 1996. Coronavirus transcription mediated by sequences flanking the transcription consensus sequence. *Virology* **217**:311–322.
- Joo, M., and S. Makino. 1992. Mutagenic analysis of the coronavirus intergenic consensus sequence. *J. Virol.* **66**:6330–6337.
- Joo, M., and S. Makino. 1995. The effect of two closely inserted transcription consensus sequences on coronavirus transcription. *J. Virol.* **69**:272–280.
- Kim, Y.-N., Y. S. Jeong, and S. Makino. 1993. Analysis of *cis*-acting sequences essential for coronavirus defective interfering RNA replication. *Virology* **197**:53–63.
- Kim, Y.-N., M. M. C. Lai, and S. Makino. 1993. Generation and selection of coronavirus defective interfering RNA with large open reading frame by RNA recombination and possible editing. *Virology* **194**:244–253.
- Kim, Y.-N., and S. Makino. 1995. Characterization of a murine coronavirus defective interfering RNA internal *cis*-acting replication signal. *J. Virol.* **69**:4963–4971.
- Lai, M. M. C., R. S. Baric, P. R. Brayton, and S. A. Stohlman. 1984. Characterization of leader RNA sequences on the virion and mRNAs of mouse hepatitis virus, a cytoplasmic RNA virus. *Proc. Natl. Acad. Sci. USA* **81**:3626–3630.
- Lai, M. M. C., P. R. Brayton, R. C. Armen, C. D. Patton, C. Pugh, and S. A. Stohlman. 1981. Mouse hepatitis virus A59: mRNA structure and genetic localization of the sequence divergence from hepatotropic strain MHV-3. *J. Virol.* **39**:823–834.
- Lai, M. M. C., C. D. Patton, R. S. Baric, and S. A. Stohlman. 1983. Presence of leader sequences in the mRNA of mouse hepatitis virus. *J. Virol.* **46**:1027–1033.
- Lai, M. M. C., and S. A. Stohlman. 1978. RNA of mouse hepatitis virus. *J. Virol.* **26**:236–242.
- Lee, H.-J., C.-K. Shieh, A. E. Gorbalenya, E. V. Eugene, N. La Monica, J. Tuler, A. Bagdzhadzhyan, and M. M. C. Lai. 1991. The complete sequence (22 kilobases) of murine coronavirus gene 1 encoding the putative proteases and RNA polymerase. *Virology* **180**:567–582.
- Leibowitz, J. L., K. C. Wilhelmsen, and C. W. Bond. 1981. The virus-specific intracellular RNA species of two murine coronaviruses: MHV-A59 and MHV-JHM. *Virology* **114**:39–51.
- Liao, C.-L., and M. M. C. Lai. 1995. A *cis*-acting viral protein is not required for the replication of a coronavirus defective-interfering RNA. *Virology* **209**:428–436.
- Lin, Y.-J., and M. M. C. Lai. 1993. Deletion mapping of a mouse hepatitis virus defective interfering RNA reveals the requirement of an internal and discontinuous sequence for replication. *J. Virol.* **67**:6110–6118.
- Makino, S., M.-F. Chang, C.-K. Shieh, T. Kamahora, D. M. Vannier, S. Govindarajan, and M. M. C. Lai. 1987. Molecular cloning and sequencing of a human hepatitis delta virus RNA. *Nature (London)* **329**:343–346.
- Makino, S., N. Fujioka, and K. Fujiwara. 1985. Structure of the intracellular defective viral RNAs of defective interfering particles of mouse hepatitis virus. *J. Virol.* **54**:329–336.
- Makino, S., M. Joo, and J. K. Makino. 1991. A system for study of coronavirus mRNA synthesis: a regulated, expressed subgenomic defective interfering RNA results from intergenic site insertion. *J. Virol.* **65**:6031–6041.
- Makino, S., and M. M. C. Lai. 1989. High-frequency leader sequence switching during coronavirus defective interfering RNA replication. *J. Virol.* **63**:5285–5292.
- Makino, S., C.-K. Shieh, L. H. Soe, S. Baker, and M. M. C. Lai. 1988. Primary structure and translation of a defective interfering RNA of murine coronavirus. *Virology* **166**:550–560.
- Makino, S., L. H. Soe, C.-K. Shieh, and M. M. C. Lai. 1988. Discontinuous transcription generates heterogeneity at the leader fusion sites of coronavirus mRNAs. *J. Virol.* **62**:3870–3873.
- Makino, S., F. Taguchi, N. Hirano, and K. Fujiwara. 1984. Analysis of genomic and intracellular viral RNAs of small plaque mutants of mouse hepatitis virus, JHM strain. *Virology* **139**:138–151.
- Makino, S., K. Yokomori, and M. M. C. Lai. 1990. Analysis of efficiently packaged defective interfering RNAs of murine coronavirus: localization of a possible RNA-packaging signal. *J. Virol.* **64**:6045–6053.
- Masters, P. S., C. A. Koetzner, C. A. Kerr, and Y. Heo. 1994. Optimization of targeted RNA recombination and mapping of a novel nucleocapsid gene mutation in the coronavirus mouse hepatitis virus. *J. Virol.* **68**:328–337.
- Pachuk, C. J., P. J. Bredenbeek, P. W. Zoltick, W. J. M. Spaan, and S. R. Weiss. 1989. Molecular cloning of the gene encoding the putative polymerase of mouse hepatitis virus, strain A59. *Virology* **171**:141–148.
- Repass, J. F., and S. Makino. Unpublished data.
- Sawicki, S. G., and D. L. Sawicki. 1986. Coronavirus minus-strand RNA synthesis and effect of cycloheximide on coronavirus RNA synthesis. *J. Virol.* **57**:328–334.
- Sawicki, S. G., and D. L. Sawicki. 1990. Coronavirus transcription: subgenomic mouse hepatitis virus replicative intermediates function in RNA synthesis. *J. Virol.* **64**:1050–1056.
- Schaad, M. C., and R. S. Baric. 1994. Genetics of mouse hepatitis virus transcription: evidence that subgenomic negative strands are functional templates. *J. Virol.* **68**:8169–8179.
- Sethna, P. B., M. A. Hofmann, and D. A. Brian. 1991. Minus-strand copies of replicating coronavirus mRNAs contain antileaders. *J. Virol.* **65**:320–325.
- Sethna, P. B., S.-L. Hung, and D. A. Brian. 1989. Coronavirus subgenomic minus-strand RNAs and the potential for mRNA replicons. *Proc. Natl. Acad. Sci. USA* **86**:5626–5630.
- Shaklee, P. N. 1990. Negative-strand RNA replication by Q β and MS positive-strand RNA phage replicases. *Virology* **178**:340–343.
- Spaan, W., H. Delius, M. Skinner, J. Armstrong, P. Rottier, S. Smeekens, B. A. M. van der Zeijst, and S. G. Siddell. 1983. Coronavirus mRNA synthesis involves fusion of non-contiguous sequences. *EMBO J.* **2**:1939–1944.
- Tousch, D., M. Jacquemond, and M. Tepfer. 1994. Replication of cucumber mosaic virus satellite RNA from negative-sense transcripts produced either in vitro or in transgenic plants. *J. Gen. Virol.* **75**:1009–1014.
- van der Most, R. G., P. J. Bredenbeek, and W. J. M. Spaan. 1991. A domain at the 3' end of the polymerase gene is essential for encapsidation of coronavirus defective interfering RNAs. *J. Virol.* **65**:3219–3226.
- van der Most, R. G., R. J. de Groot, and W. J. M. Spaan. 1994. Subgenomic RNA synthesis directed by a synthetic defective interfering RNA of mouse hepatitis virus: a study of coronavirus transcription initiation. *J. Virol.* **68**:3656–3666.
- van der Most, R. G., L. Heijnen, W. J. M. Spaan, and R. J. de Groot. 1992. Homologous RNA recombination allows efficient introduction of site-specific mutations into the genome of coronavirus MHV-A59 via synthetic co-replicating RNAs. *Nucleic Acids Res.* **20**:3375–3381.
- van der Werf, S., J. Bradley, E. Wimmer, F. W. Studier, and J. J. Dunn. 1986. Synthesis of infectious poliovirus RNA by purified T7 RNA polymerase. *Proc. Natl. Acad. Sci. USA* **83**:2330–2334.
- Weis, J. H. 1994. Race no more: an alternative approach to cloning the 5' end of transcripts. *Nucleic Acids Res.* **22**:3427–3428.
- Winship, P. R. 1989. An improved method for directly sequencing PCR material using demethyl sulfoxide. *Nucleic Acids Res.* **17**:1266.